Flow Characteristics of Three-Dimensional Wall Jets

Allan T. Kirkpatrick, Ph.D.
Member ASHRAE

Allen E. Kenyon

ABSTRACT

The subject of this paper is the experimental determination of the flow characteristics of three-dimensional wall jets. The jets were produced from a diffuser with a rectangular outlet. The diffuser outlet size and flow rate were varied to produce both low and high outlet aspect ratios and Reynolds numbers. Velocity profile measurements were made to determine the centerline velocity decay and the extent of the lateral and vertical spread of the jet. Using a simple jet model, the velocity decay coefficients, virtual origins, and spread angles were deduced and compared with previously published results for smaller laboratory-scale jets.

INTRODUCTION

The subject of this paper is the behavior of three-dimensional wall jets produced by a room air diffuser with a rectangular outlet. Wall or ceiling jets are commonly used for diffusing the momentum of the supply air from the diffuser to prevent drafts in the occupied zone of an enclosed space. The diffusion of the jet is characterized by the centerline velocity decay coefficient and the lateral and vertical half-widths. In this paper, measurements are made of the maximum centerline velocity profiles for two outlet heights and two volume flow rates at each height. The lateral and vertical jet half-widths are also measured for the two flow rates at each outlet height. These measurements are made with outlet aspect ratios and Reynolds numbers similar to those used by Sforza and Herbst (1970) in wall jet measurements with smaller laboratory-scale outlets. The study in this paper makes use of a ceiling diffuser with a rectangular outlet sized for use in HVAC applications. Beyond a comparison of the general nature of the velocity decay and jet spread measured in this study and the Sforza and Herbst study, a simple jet model is used to obtain jet flow characteristics from the data. These characteristics are the centerline velocity decay coefficient, K, the virtual origin of the jet in reference to the diffuser outlet, x_p, and the spread angles of the jets laterally (parallel to the ceiling) and vertically (perpendicular to the ceiling), β_l and β_v.

JET DIFFUSION CHARACTERISTICS

A wall jet produced by a diffuser with a rectangular outlet of finite aspect ratio AR is a three-dimensional jet. The jet velocity in the x-direction can vary in the axial or centerline (x), the vertical (y), and the lateral (z) directions, at least in some region downstream of the outlet. It is common to refer to three axial regions for this type of jet. Closest to the outlet is the potential core, or Zone 1, of the jet, where the velocity remains equal to the outlet velocity. The next region is the characteristic decay region, or Zone 2, starting where the velocity begins to decay from its initial value. Here the velocity decay depends on the outlet geometry and is often represented as a plane wall jet decay where the lateral width is large compared with the height of the opening. The outermost region is termed the axial or radial decay region, or Zone 3, where the velocity decay is similar to that of a radial jet (ASHRAE 1993; Engel and Kirkpatrick 1993).

Some variables characterizing a wall jet are presented in Figure 1, which are used to obtain an expression for the jet centerline velocity in Zone 3. The centerline distance x is measured from the diffuser outlet. The y-axis is perpendicular to the ceiling and the z-axis is oriented laterally, as shown in the figure. The maximum centerline velocity u_m is measured at y_m, and one-half this maximum velocity, $1/2u_m$, is measured at the half-width $y_{m/2}$. The virtual origin is the point on the x axis from which the jet appears to originate, when the line connecting the half-widths is extended back to the axis. The virtual origin is a distance x_p from the diffuser outlet. The

Allan Kirkpatrick is a professor in the Mechanical Engineering Department, Colorado State University, Fort Collins. **Allen Kenyon** is an engineer with Symbios Logic, Fort Collins, Colo.

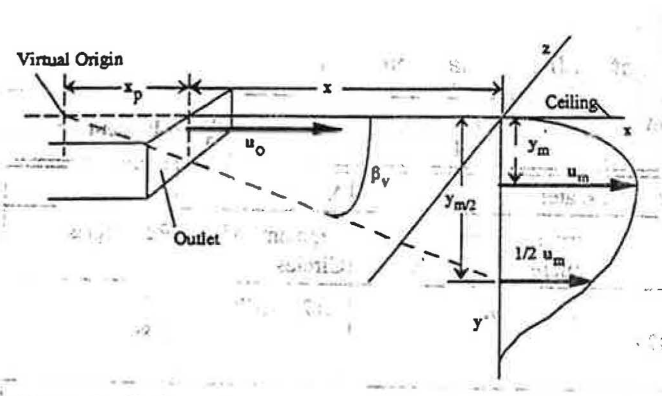

Figure 1 Schematic of a wall jet with velocities and distances.

angle β_v is measured between the line connecting the half-widths and the x axis. Although not shown in Figure 1, the jet also spreads laterally, or in the z direction, and the half maximum velocity $1/2u_m$ is measured at the lateral half-width $z_{m/2}$ on either side of the x axis.

Analysis indicates that in Zone 2 the centerline velocity u_m is proportional to $x^{-1/2}$, and in Zone 3, u_m is proportional to x^{-1} (ASHRAE 1993). In Zone 3, a nondimensional expression for the maximum centerline velocity u_m at a given value of x is

$$\frac{u_m}{u_o} = K\frac{A_o^{1/2}}{x + x_p}, \tag{1}$$

where K is the velocity decay coefficient equal to the product of the nondimensional jet velocity and distance from the outlet, u_o is the effective outlet velocity, and A_o is the effective outlet area, defined from the Bernoulli equation and the continuity equation (Koestel 1957) as

$$u_o = \left(\frac{2\Delta p_{st}}{\rho}\right)^{1/2} \tag{2}$$

$$A_o = \frac{Q}{u_o} \tag{3}$$

The quantity Δp_{st} is the static pressure drop measured across the diffuser outlet, ρ is the density of the air at the outlet, and Q is the volume flow rate of the air. The effective outlet velocity and area, u_o and A_o, in the velocity decay equation (Equation 1) are based on the static pressure drop. Equation 2 does not account for losses at the outlet; thus, it is an approximation that slightly overestimates the actual average outlet velocity and overestimates the actual outlet area. In Equation 1, negative values of x_p are in front of or downstream of the diffuser. Another useful characteristic parameter is the jet outlet momentum flow, M_o, equal to $\rho A_o u_o^2$.

PREVIOUS THREE-DIMENSIONAL WALL JET EXPERIMENTS

Early studies of wall jets are given in Koestel et al. (1950), Tuve (1953), and Koestel (1957). A review study that gathers and compares various three-dimensional wall jet experimental findings is that of Launder and Rodi (1981, 1983). Sforza and Herbst (1970) used a very small outlet area of 6×10^{-5} m^2 (0.1 in.^{2}), with the wall jet spreading against a very smooth, polished aluminum surface.

The outlets for other studies of three-dimensional wall jets have shapes other than rectangles or aspect ratios much different from those used for the present study. Quantities pertinent to a comparison of some different experiments, including the experiments of this study, are listed in Table 1. The outlet area reported in this case is geometric outlet area A. The Reynolds number is the outlet Reynolds number based on the outlet height (Re = hu_o/ν). Newman et al. (1972) conducted measurements on three-dimensional air and water jets issuing from circular outlets that were tangent to a flat surface. Rajaratnam and Pani (1974) measured the development of three-dimensional wall jets from orifices with square, circular, triangular, and elliptical shapes. For the water jets they used, they explored in detail the similarity of both the vertical and transverse velocity profiles, finding that these profiles were, in fact, reasonably similar for axial distances greater than about 10 times the nozzle height. They found that the centerline velocity decay at some distance from the nozzle varied as $1/x$, as radial velocity decay theory predicts. Padmanabham and Gowda (1991) used orifices of various circle segment shapes to produce air wall jets.

DESCRIPTION OF EXPERIMENT

The test room is located in a university laboratory. The room length is 7.64 m (25 ft, 1 in.), its width is 4.83 m (15 ft, 10 in.), and its height is 2.74 m (9 ft). The equipment outside the test room includes a data acquisition/control unit and a microcomputer equipped with an A/D card and data acquisition software.

Measurements are conducted with a rectangular outlet area diffuser using isothermal air. The outlet width w is 29.6 cm (11.7 in.), and measurements are made at two outlet heights h, 0.63 cm (0.25 in.) and 2.26 cm (0.89 in.). The two outlet areas A are 0.0019 m^2 (2.9 in.^{2}) and 0.0067 m^2 (10.4 in.^{2}), which are factors of 29 and 104 larger than the Sforza and Herbst outlet. A schematic of the diffuser appears in Figure 2. The outlet is formed by three sides of the diffuser and a slanting bottom plate, as shown in the figure. Having the plate hinged at the back allows for adjustment of the diffuser outlet height h. The diffuser enclosure is 28.8 cm (11.3 in.) high, measured from the plate hinge (at ceiling level) to the top of the diffuser box. The length of the diffuser, from the back to the outlet, is 30.1 cm (11.9 in.). The diffuser interior width is 29.6 cm (11.7 in.). The static pressure tap is located midway along the diffuser length, 2.9 cm (1.1 in.) above the top edge of the rectangular outlet. The ceiling level is flush with the top

TABLE 1
Parameters of Previous and Present Wall Jet Measurements

	Sforza, Herbst 1970	Newman et al. 1972	Rajaratnam, Pani 1974	Padmanabham, Gowda 1991	Present Study
Fluid	Air	Air, water	Water	Air	Air
Outlet Shapes	Rectangles	Circle	Circle, Rectangle, Square, Triangle, Ellipse	Segments of Circles	Rectangles
Outlet Height or Diameter, h (in.)	0.1 0.071 0.05	Air 0.125 Water 0.079	0.375 - 0.62	0.175 - 0.752	0.25 0.89
Outlet Length (in.)	1.0 1.414 2.0		0.25 - 0.607	0.752 segment dia.	11.7
Outlet Aspect Ratio (length/height)	10 20 40	Air 1 Water 1	Close to 1 for all shapes	1.0 - 4.3	46.6 13.1
u_o (m/s)	63	Air 77 Water 1.4	7.4 - 7.9	80	4.6 - 23
Reynolds Number	8170 5780 4090	Air 16400 Water 2800	59500 - 102000	95400	3000 - 13000
Momentum Flow (N)	0.25	Air 0.048 Water 0.0062	3.93 - 8.51	0.35 - 1.86	0.10 - 1.3
Centerline Distance to Outlet Height Ratio, x/h	5 - 300	5 - 190	1 - 85	3 - 120	13 - 720

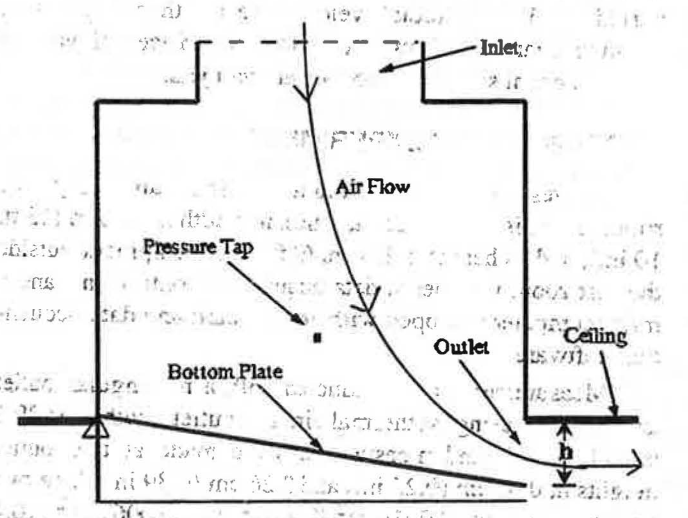

Figure 2 Diffuser cross section.

edge of the outlet. A 6-inch-diameter duct brings air from an air handler into the diffuser. A diffusion screen placed horizontally inside the diffuser produces a uniform outlet velocity (± 0.1 m/s for a nominal velocity of 5 m/s) in the lateral direction.

A schematic showing the diffuser in the ceiling, the air handler, and the duct is shown in Figure 3. The figure shows the positions of the duct thermocouple and velocity probe for the calculation of flow rate, the velocity probe in the room, and the pressure taps in the diffuser and the room, along with the instruments into which the signals from these devices are directed. The maximum centerline velocity u_m along the length of the room and the lateral and vertical half-widths $z_{m/2}$ and $y_{m/2}$ are measured for the jets at eight centerline positions downstream of the diffuser. There are centerline velocity data accompanying both the lateral and the vertical half-width data, since the half-width measurements in each case require knowledge of the magnitude of the velocity u_m. The jet centerline velocity u_m and velocities u along vertical and transverse lines from the centerline are measured with a constant-temperature omnidirectional thermal anemometer. The omnidirectional probe is sensitive to the transverse turbulent velocity components as well as the streamline components; however, the streamline components are assumed to be the dominant velocity components. The anemometer is placed on a stand with wheels. The voltages from this instrument are fed to the A/D card in the computer for averaging. The flow rate Q of the air is adjusted manually at the air-handler outlet. The flow rate is determined from an anemometer inserted into the supply air duct and corrected for the airstream temperature.

The static pressure difference Δp_{st} across the diffuser outlet is measured by a pressure transducer. One pressure tap is placed flush with the diffuser wall, and the other tap is located in the room next to a wall. The jet or probe temperature T_p is obtained by a type-T thermocouple placed about 1.5 cm to the side of the velocity probe in the room. The average room temperature T_r comes from the average of four type-T thermocouples placed on the surfaces of the four room walls at

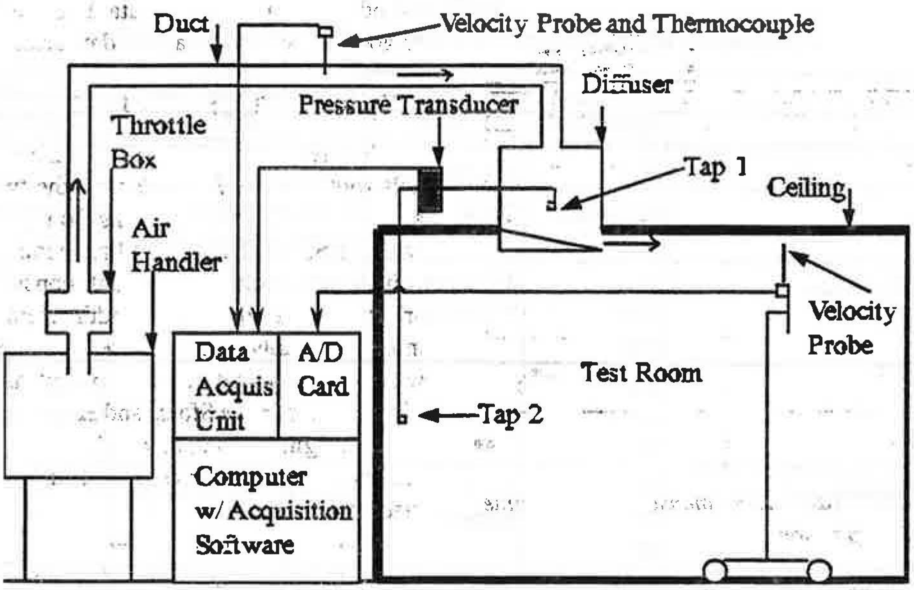

***Figure 3** Schematic of air handler, duct, diffuser, test room, and instrumentation.*

their midpoints. The effective outlet velocity u_o is calculated from the measured static pressure drop across the diffuser outlet and the calculated air density.

The velocity readings are averages of 1,000 samples of the instantaneous velocity taken at a 20-Hz rate. Both the average velocity and the standard deviation σ from the average are displayed after a 50-second measurement interval. Moving averages of the static pressure difference and the flow rate are obtained so that the final average displayed is the average of the readings taken during the velocity-averaging process. The temperature readings are single instantaneous readings.

In order to find the lateral and vertical positions where the maximum velocity u_m is measured at each x position, velocity profiles are first obtained laterally and vertically at several x positions. These positions vary very little with flow rate. In the lateral direction, the maximum velocity u_m is found to occur on the centerline of the room, coinciding with a line bisecting the rectangular outlet. To obtain the lateral or the vertical half-width measurements, three 50-second measurement periods are run at each position x. The first measurement is made to obtain u_m. Before the second and third measurements are taken, the probe is positioned so that the velocity reading is approximately $1/2u_m$. Two 50-second measurements are then taken at locations where the measured velocities are greater than, and less than, $1/2u_m$, respectively. A linear interpolation using these two velocities gives the velocity $1/2u_m$ and the half-width. In this process, for each outlet height and flow rate used, data are obtained separately for centerline velocities and lateral half-widths and for centerline velocities and vertical half-widths.

Parameters for the experiments are shown in Table 2. Outlet height, aspect ratio, flow rate, effective outlet velocity and area, and outlet Reynolds number are shown for both the

TABLE 2
Experiment Parameters

Experiments	h		AR	Q		u_o	A_o	Re
	(in.)	(cm)		(cfm)	(m^3/s)	(m/s)	(m^2)	
Centerline Lateral	0.25	0.63	46.6	30	0.014	9.36	0.00152	3000
				90	0.042	23.1	0.00186	7400
	0.89	2.26	13.1	50	0.024	4.56	0.00520	5200
				150	0.071	11.3	0.00629	13000
Centerline Vertical	0.25	0.63	46.6	30	0.014	9.32	0.00154	3000
				90	0.042	22.3	0.00188	7200
	0.89	2.26	13.1	50	0.024	4.59	0.00517	5300
				150	0.071	11.4	0.00624	13000

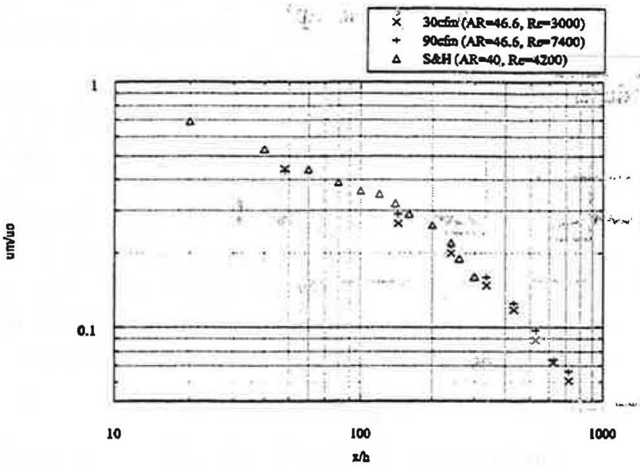

Figure 4 *High aspect ratio nondimensional centerline velocity comparison.*

centerline-lateral and centerline-vertical sets of measurements.

JET CENTERLINE VELOCITY RESULTS

Figure 4 plots the nondimensional velocity u_m/u_o vs. the centerline coordinate x/h for the high aspect ratio 0.25-inch outlet and the high aspect ratio Sforza and Herbst data. The Sforza and Herbst data were published in terms of x/h, so the data in this paper are plotted in a similar fashion. For the diffuser used in these experiments, the effective area A_o is essentially equal to the geometric area $A = hw$ (w is the width of the diffuser outlet). Thus, the diffuser height h is an acceptable surrogate for the characteristic length $A_o^{1/2}$. In their study, Sforza and Herbst took the four points farthest from the outlet and fit a line through them with a $1/x$ type decay. Figure 5 plots u_m/u_o vs. x/h for the low aspect ratio 0.89-inch outlet measurements and the Sforza and Herbst low aspect ratio measurements. Overall, there is remarkable agreement in the Zone 3 velocities for the two studies, beginning at about x/h of 200 for the high aspect ratio data and at about 40 for the low aspect ratio data. Only the lower Reynolds number data of the present study's low aspect ratio do not coincide very well with the other low aspect ratio data. In Zone 2 the agreement is not as good between the various data sets.

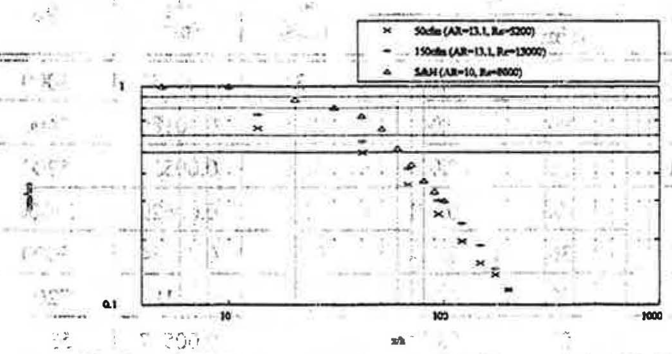

Figure 5 *Low aspect ratio nondimensional centerline velocity comparison.*

JET HALF-WIDTH RESULTS

Figures 6 and 7 are plots of the nondimensional lateral half-widths $z_{m/2} / h$ vs. x/h from the two studies. The higher aspect ratio lateral half-widths from this study compare well with the Sforza and Herbst half-widths, at least in that both half-widths remain somewhat constant until x/h reaches around 200. Then the half-widths from both studies increase more noticeably. For the lower aspect ratio, the lateral half-widths of this study do not exhibit as strong a neck-down effect as seen in the Sforza and Herbst half-widths close to the outlet. Beginning at $x/h = 50$, the Sforza and Herbst data display a curvature very similar to that of the data of this study that extend past $x/h = 100$.

The nondimensional vertical half-widths $y_{m/2} / h$ are plotted vs. x/h in Figures 8 and 9 for both studies. The higher aspect ratio vertical half-widths from this study not only display good similarity with one another but also with the

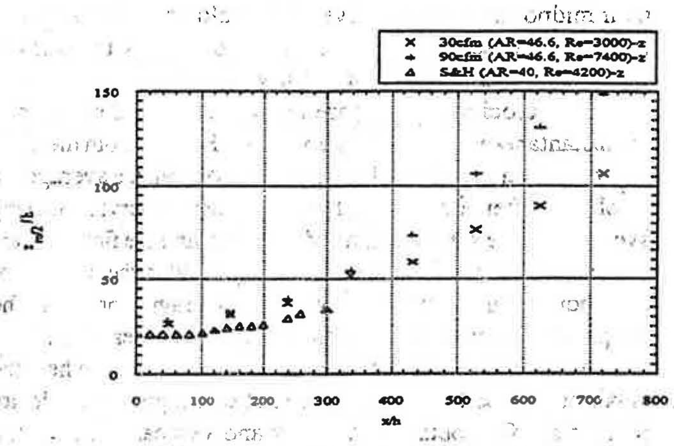

Figure 6 *High aspect ratio nondimensional lateral half-width comparison.*

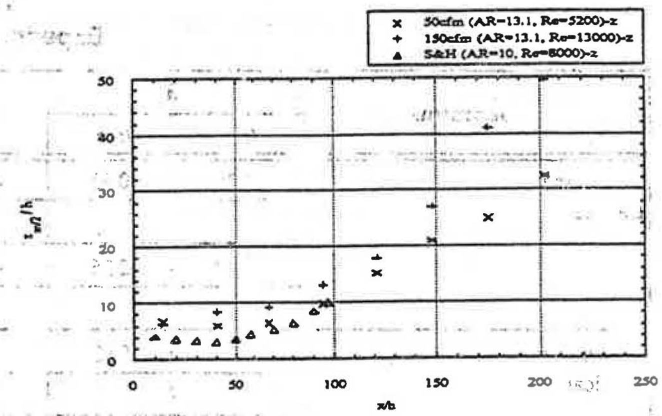

Figure 7 *Low aspect ratio nondimensional lateral half-width comparison.*

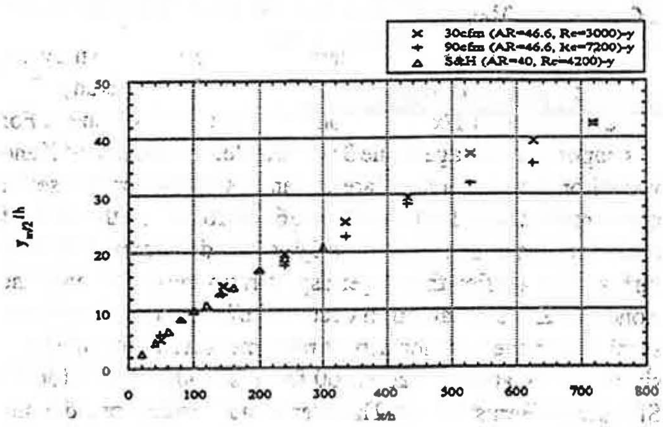

Figure 8 High aspect ratio nondimensional vertical half-width comparison.

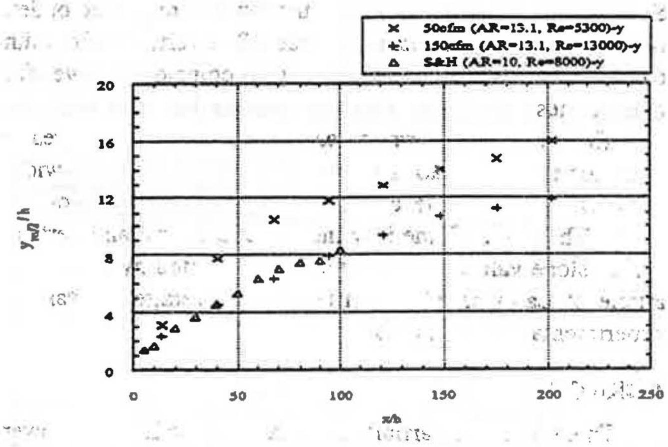

Figure 9 Low aspect ratio nondimensional vertical half-width comparison.

Sforza and Herbst half-widths. For the lower aspect ratio measurements, there is also very good similarity shown between the high Reynolds number vertical half-widths and Sforza and Herbst half-widths. The low Reynolds number half-widths of Figure 9 at least fall along a similarly sloped curve to that of the other data, even leveling a bit with the other data at larger centerline distances.

The influence of the room dimensions on the jet is small for the present study, since the largest x distance is 4.6 m, which is 0.9 m less than 1.5 times the square root of the cross-sectional area of the room (ASHRAE 1993). A comparison of Figures 6 and 7 with Figures 8 and 9 shows the opposing manner in which the jets spread in the two transverse directions. While the lateral spread rate becomes more pronounced with centerline distance from the outlet, the vertical spread rate becomes less pronounced with centerline distance.

JET DECAY CHARACTERISTICS

The measured lateral and vertical jet velocity spread and centerline velocity decay are now quantified by calculating the spread angles β_l and β_v, the velocity decay coefficients K, and the virtual origins x_p. By inspection of Figures 4 and 5, the two half-width points measured closest to the diffuser are omitted for each data set, since they are in the Zone 2 region. Lines of the form $z_{m/2} / h = a + b\ (x/h)$ or $y_{m/2} / h = c + d\ (x/h)$ are fit to the remaining data of Figures 6 through 9. When this is done, the slopes of the equations equal the tangent of the spread angle β_l or β_v. The slopes and angles for both the lateral and vertical spread are given in Table 3. The jet spread is greater in the lateral than in the vertical direction. Table 3 also lists the values for the slopes of the spread as obtained from averages of several previous three-dimensional jet experiments (Launder and Rodi 1983). There is remarkable agreement between the average slopes of the present data and the values of Launder and Rodi: 0.22 and 0.26, respectively, for the lateral slopes (a 15% difference) and 0.043 and 0.048, respectively, for the vertical slopes (a 10% difference).

Figure 10 plots the nondimensional quantities $x / (A_o)^{1/2}$ vs. u_o/u_m for the centerline-lateral measurements. The velocity decay constants and virtual origins are found from Equation 1, solved for $x / (A_o)^{1/2}$:

TABLE 3
Slopes and Spread Angles for Lines Connecting Half-Width Data

Experiment	h (in.)	Q (m³/s)	Half-Width Slope	β_l (deg.)	β_v (deg.)	Launder and Rodi Half-Width Slope
Centerline Lateral	0.25	0.014	0.14	7.9		0.26
		0.042	0.24	13		
	0.89	0.024	0.19	11		
		0.071	0.31	17		
Centerline Vertical	0.25	0.014	0.048		2.8	0.048
		0.042	0.049		2.8	
	0.89	0.024	0.035		2.0	
		0.071	0.041		2.4	

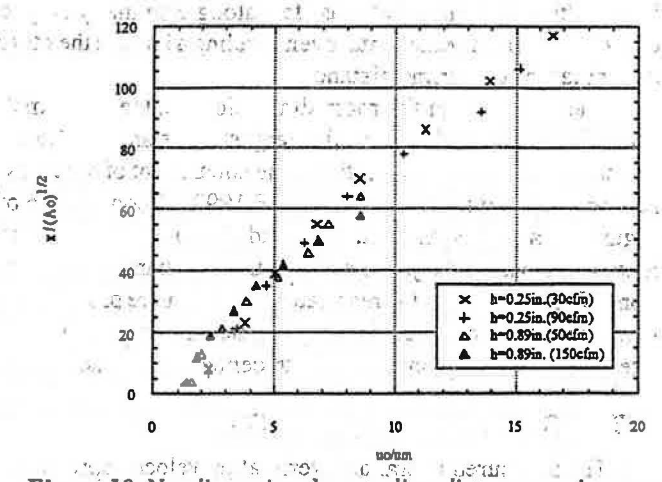

Figure 10 Nondimensional centerline distance vs. inverse velocity.

$$\frac{x}{A_o^{1/2}} = K\frac{u_o}{u_m} - \frac{x_p}{A_o^{1/2}} \qquad (4)$$

Linear equations of the form $y = a + bx$ are fit to the data of Figure 10, where the slope is K and the y-intercept is $-x_p / (A_o)^{1/2}$. The intercept value $(-x_p / (A_o)^{1/2})$ is solved for x_p, using the effective outlet areas of Table 2. The results for K and x_p are shown in Table 4. Included in the table are results of the identical analysis as described above, done on the centerline-vertical measurements. The negative sign of the x_p values indicates that the virtual origins lie downstream of the diffuser outlet. The calculated uncertainties for the decay coefficients, δK, and virtual origins, δx_p, are listed as well. The larger uncertainty at $h = 0.89$ in., $Q = 50$ cfm, occurs because the fixed pressure transducer uncertainty is a considerably larger percentage of the pressure drop measured for this case than it is for the other three cases. However, the actual measured variation in the pressure readings for the $h = 0.89$ in., $Q = 50$ cfm is not nearly as large (standard deviation / average value = 0.46%).

CONCLUSIONS

The jet diffusion characteristics of the present study are very similar to those of the Sforza and Herbst study. The velocity varies as $1/x^{1/2}$ for Zone 2 and as $1/x$ for Zone 3. For this paper, the average Zone 3 velocity decay coefficient K and virtual origin location x_p are 6.7 and −0.32 m for one set of measurements and 6.6 and −0.36 m for the other set of measurements. The virtual origins lie downstream of the diffuser outlet. For the larger aspect ratio measurements, the Zone 2 to Zone 3 transition occurs at x/h of about 200 in both studies. For the smaller aspect ratio measurements, the transition occurs at x/h of about 60 for this study and 40 for the Sforza and Herbst study. The lateral and vertical spread of the jets with centerline distance for this study is similar to the spread for the Sforza and Herbst study. The neck-down or decreasing lateral half-width development, measured by Sforza and Herbst at low x/h for the lower aspect ratio outlet, is not observed in the data of this study. The vertical half-width data for the higher aspect ratio outlet jets coincide very well for both studies.

The measured lateral spread is about five times greater than the vertical spread. The average Zone 3 lateral half-width slope is 0.22, and the average vertical half-width slope is 0.043. This is confirmed by the average lateral and vertical spread slope values of 0.26 and 0.048 reported by the review article of Launder and Rodi (1983) as averages of various experimental study results.

ACKNOWLEDGMENTS

This work was partially supported by the Electric Power Research Institute (EPRI). The EPRI contract monitors are Mr. Ronald Wendland and Mr. Mukesh Khattar.

NOMENCLATURE

A = geometric diffuser outlet area (m^2)
A_O = effective outlet area (m^2)
AR = outlet aspect ratio
h = one-way diffuser outlet height (in.)

TABLE 4
Velocity Data Decay Coefficients, Virtual Origins, and Uncertainty

Experiment	h (in.)	AR	Q (m^3/s)	u_o (m/s)	A_o (m^2)	Re	M_o (N)	K	x_p (m)	δK and δx_p(%)
Centerline Lateral	0.25	46.6	0.014	9.4	0.00152	3000	0.13	6.6	−0.37	3.6
			0.042	23.1	0.00186	7400	0.96	6.4	−0.37	2.9
	0.89	13.1	0.024	4.6	0.00520	5200	0.10	7.4	−0.03	9.2
			0.071	11.3	0.00629	13000	0.78	6.3	−0.51	3.2
Centerline Vertical	0.25	46.6	0.014	9.3	0.00154	3000	0.13	7.1	−0.21	3.6
			0.042	22.3	0.00188	7200	0.91	5.8	−0.60	2.9
	0.89	13.1	0.024	4.6	0.00517	5300	0.10	6.7	−0.31	9.2
			0.071	11.4	0.00624	13000	0.76	6.8	−0.32	3.2

K = velocity decay coefficient

δK = uncertainty in velocity decay coefficient (%)

M_o = jet outlet momentum flow (N)

Δp_{st} = static pressure difference across diffuser outlet (Pa)

Q = volumetric flow rate (m^3/s)

Re = diffuser outlet Reynolds number based on outlet height

T_p = temperature at the velocity probe (°C)

T_r = average temperature in the test room (°C)

u = jet velocity in the x direction (m/s)

u_o = effective outlet velocity (m/s)

u_m = maximum centerline x-direction velocity at a given x position (m/s)

w = fixed width of diffuser outlet (in.)

x = centerline coordinate, measured from the diffuser outlet (m)

x_p = distance from the diffuser outlet to the virtual origin of the jet (m)

δxp = uncertainty in distance from the diffuser outlet to the virtual origin (%)

y = vertical coordinate measured from ceiling (m)

y_m = vertical distance from ceiling to position where u_m is measured (m)

$y_{m/2}$ = vertical distance from ceiling to position where $u_m/2$ is measured (m)

z = lateral coordinate from centerline (m)

$z_{m/2}$ = lateral distance from centerline to position where $u_m/2$ is measured (m)

β_l = jet spread angle between centerline and line connecting $z_{m/2}$ positions),

β_v = jet spread angle between centerline and line connecting $y_{m/2}$ positions (°)

ρ = density of the air at the outlet (kg/m^3)

σ = standard deviation of the velocity measurements (m/s)

REFERENCES

ASHRAE. 1993. *1993 ASHRAE Handbook—Fundamentals*. Atlanta: American Society of Heating, Refrigerating and Air-Conditioning Engineers, Inc.

Engel, J., and A. Kirkpatrick. 1993. Experimental determination of the airflow performance of a variable area radial diffuser. *ASHRAE Transactions* 99(2): 759-769.

Koestel, A., P. Hermann, and G. Tuve. 1950. Comparative study of ventilating jets from various types of outlets. *ASHVE Transactions* 56: 459-478.

Koestel, A. 1957. Jet velocities from radial flow outlets. *ASHRAE Transactions* 63: 505-526.

Launder, B., and W. Rodi. 1981. The turbulent wall jet. *Progress in Aerospace Sciences* 19: 81-128.

Launder, B., and W. Rodi. 1983. The turbulent wall jet—Measurements and modeling. *Annual Review of Fluid Mechanics* 15: 429-459.

Newman, B. G., et al. 1972. Three-dimensional wall jet originating from a circular orifice. *Aeronautical Quarterly* 23: 188-200.

Padmanabham, G., and B. Gowda. 1991. Mean and turbulence characteristics of a class of three-dimensional wall jets—Part 1: Mean flow characteristics. *Transactions of the ASME* 113: 620-628.

Rajaratnam, N., and B. Pani. 1974. Three-dimensional turbulent wall jets. *ASCE Journal of the Hydraulics Division* 100: 69-83.

Sforza, P., and G. Herbst. 1970. A study of three-dimensional, incompressible, turbulent wall jets. *AIAA Journal* 8: 276-283.

Tuve, G. 1953. Air velocities in ventilating jets. ASHVE Transactions 59: 261-282.